Int. J. Electrochem. Sci., 14 **(2019)** 1782 – 1793, doi: 10.20964/2019.02.26

International Journal of
ELECTROCHEMICAL
SCIENCE
www.electrochemsci.org

A High-Performance Supercapacitor Based on Nitrogen-Doped Porous Carbon Derived from Cycas Leaves

Chaochao Xu, Fen Xu[*], *Lixian Sun*[*], *Lizhi Cao, Fang Yu, Huanzhi Zhang, Erhu Yan, Hongliang Peng, Hailiang Chu, Yongjin Zou*

Guangxi Key Laboratory of Information Materials, Guangxi Collaborative Innovation Center of Structure and Property for New Energy and Materials, School of Material Science and Engineering, Guilin University of Electronic Technology, Guilin, 541004, P. R. China
[*]E-mail: xufen@guet.edu.cn or 1732211579@qq.com, sunlx@guet.edu.cn

Received: 23 October 2018 / *Accepted:* 28 November 2018 / *Published:* 5 January 2019

In this work, we proposed a new way to synthesize nitrogen-doped porous carbon materials. Nitrogen-doped porous carbon materials were prepared using cycas leaves as the carbon source and urea as the nitrogen source. Namely, the dried cycas leaves were first burned at 300 °C and then activated by KOH containing urea at 700 °C. The prepared samples display high specific surface areas; the highest specific surface area and largest total pore volumes are approximately 2628 $m^2 g^{-1}$ and 1.39 $cm^3 g^{-1}$, respectively. A supercapacitor made by nitrogen-doped porous carbon shows attractive capacitive performance. Taking CU2-700 as an example, its specific capacitance is 373 F/g at 0.5 A/g, and 89% specific capacitance retention is reached after 10000 cycles in a three-electrode system. In addition, high specific capacitances of 260 F/g at 0.5 A/g and 203 F/g at 10 A/g are obtained, and CU2-700 has excellent cycling stability (85% specific capacitance retention after 10000 cycles at 5 A/g) in a two-electrode system. Furthermore, the energy density of the supercapacitor is approximately 9.13 W h/kg at 125 W/kg power density in a two-electrode system. These results indicate that cycas leaves are a good biomass carbon material for preparing high-performance supercapacitors.

Keywords: cycas leaves; porous carbon; urea; KOH activation; supercapacitors

1. INTRODUCTION

It is of great importance to develop sustainable equipment due to increasing fossil fuel consumption and greenhouse gas emissions. Supercapacitors, also known as electrochemical capacitors or ultra-capacitors, have attracted much attention because of their high-power energy, long cycle life, high efficiency, wide range of operating temperatures, environmental friendliness and good stability [1-6]. Based on the energy storage mechanism, supercapacitors can be divided into two categories: electric double-layer capacitors (EDLCs) with carbon-based electrodes and pseudocapacitors with metal oxide

or conducting polymer electrodes. In principle, EDLCs rely on the separation of charged species in an electrical double layer across the electrode/electrolyte interface to store energy [7]. In other words, the capacitance performance of EDLCs is mainly dependent on the electrode materials. Therefore, high surface area and suitable pores are important to EDLCs. Among various electrode materials, carbon-based materials, including activated carbons (ACs) [8], carbon fibres [9], carbon aerogels [10], carbon nanotubes [11] and graphene [12], are considered prospective electrode materials due to their high specific surface area, abundance, excellent electrical conductivity, low cost and high chemical stability.

Activated carbon was usually prepared by a two-step process; namely, the precursor was first carbonized at an appropriate temperature in an inert atmosphere and then activated by a chemical or physical method. Among them, the KOH activation method is a well-established route to obtain an appropriate pore size distribution by changing the activation temperature, time and KOH/precursor mass ratio [13,14]. However, the specific capacitance of a supercapacitor based on activated carbons is still low. To further improve the specific capacitance, an effective way is to bring heteroatoms (such as N, O, P, S or B) into the carbon to improve its electrochemical activity and energy density. Among them, N-doped porous carbons have been demonstrated to be an effective method [15-17]. Currently, biomaterials, as carbon sources for preparation of ACs, have attracted worldwide attention from an environmental point of view. To date, various biomass materials, such as shaddock peel [18], plane tree fluff [19], cotton [20] and lotus stems [21], have been used as precursors to produce ACs. It is well known that cycas is a species of plant in the family Cycadaceae that is widely distributed in China, Japan, the Philippines and Indonesia. Cycas leaves can be easily obtained every year. Cycas leaves can be a carbon precursor as a cheap, abundant, and sustainable biological resource. To the best of our knowledge, however, there is no report on the use of cycas leaves as precursors to synthesize ACs.

In this study, we develop an efficient and simple strategy to fabricate nitrogen-doped porous carbons (N-PCs) using cycas leaves as the carbon source and urea as the nitrogen source. As a result, as-made N-PCs show very high specific surface areas and high specific capacitance. This research result implies that cycas leaves can act as a new biomass source to prepare high-performance supercapacitors.

2. EXPERIMENTAL

2.1. Preparation of N-doped porous carbons

Cycas leaves were obtained from the local campus and washed, cut into short rods with a length of 1~2 cm and dried at 80 °C. The dried cycas leaves were heated to 300 °C at a heating rate of 3 °C min^{-1} and held for 2 h in a muffle furnace. The pyrolytic cycas leaves were denoted as precursor C. Nitrogen-doped porous carbons (N-PCs) were prepared by chemical activation using KOH as an activating agent and urea as a nitrogen source. The precursor C, KOH and urea in a weight ratio of 1: 2: x (x = 1, 2 or 3) were dissolved in 30 ml of deionized water under magnetic stirring and stirred for 2 h at room temperature. The mixtures were dried at 80 °C and heated at 700 °C under a N_2 atmosphere for 2 h. The products were washed using 1 M HCl solution and deionized water and then dried overnight at 100 °C. The product was denoted as CUx-700, where x (x = 1, 2 or 3) stands for the weight ratio of the

precursor C and urea. For comparison, C-700 was prepared by using the same procedures as those of CUx-700, except for no urea.

2.2. Material characterization

The morphology and microstructure of the material were characterized by scanning electron microscopy (SEM, JSM-6360LV, EOL Ltd., Japan) equipped with X-Max20 energy dispersive X-ray spectroscopy (EDS). The crystalline nature and phase purity of the samples were investigated by powder X-ray diffraction (XRD, Bruker-D8 Advance diffractometer (Germany) with Cu Kα radiation). Raman characterization of the N-PCs was carried out by laser confocal Raman spectroscopy (Lab RAMHR Evolution, Horiba JY, France) employing a 532 nm laser beam. The surface functionalities and chemical composition of the N-PCs were characterized by X-ray photoelectron spectrometry (XPS, Escalab 250Xi, Thermo Fisher, USA) with Al Kα radiation. Nitrogen sorption isotherms were measured on a gas adsorption analyser (Autosorb iQ2, Quantachrome sorptometer, USA) at 77 K. Before measurement, the samples were degassed at 80 °C for 2 h and then heated at 150 °C for 10 h.

2.3. Electrochemical characterization

The working electrode was typically fabricated by grinding the N-PCs as the active material (80 wt.%), carbon black (10 wt.%) and polytetrafluoroethylene (PTFE, 10 wt.%) in water. The mixture was pressed into a disk with a diameter of 10 mm under a pressure of 6 MPa after drying under infrared light. The disk was then pressed with the nickel foam as a current collector at 8 MPa for 1 min. The electrochemical performance of the supercapacitor made by the N-PCs was studied by cyclic voltammetry (CV), galvanostatic charge-discharge (GCD) and electrochemical impedance spectroscopy (EIS). CV and GCD tests were conducted on a CHI660e electrochemical workstation (Chenhua Instrument Inc). CV measurements were carried out over the potential range from -1 to 0 V at scan rates of 5, 10, 20, 50, 100 and 200 mV/s. EIS was performed in a frequency range from 100 mHz to 100 kHz with an amplitude of 5 mV on a Zahner IM6e electrochemical workstation. The electrochemical tests were performed using a standard three-electrode system with a Hg/HgO electrode as the reference electrode and a platinum electrode as the counter electrode in a 6 M KOH electrolyte solution at 25 °C. The electrochemical performance was also measured in a two-electrode symmetric supercapacitor configuration at 25 °C. The gravimetric capacitance, gravimetric energy density and gravimetric power density were calculated using established equations [22] (for a 3-electrode and 2-electrode system) based on the mass of the active material in an electrode.

3. RESULTS AND DISCUSSION

3.1. Morphological and structural characterization

The morphologies of the as-prepared samples were characterized by scanning electron microscopy (SEM) and are summarized in Fig. 1. As shown in Fig. 1a, the precursor C from cycas leaves

has a lumpy structure without obvious pores. The C-700 obtained by activating precursor C produces many interconnected pores (see Fig. 1b). These pores are beneficial to ion transfer. In addition, after doping N in precursor C and activation, the structure of CU2-700 becomes thin slices with a wrinkle structure and has many pores on each slice (see Fig. 1c). This special structure can significantly shorten the ion diffusion paths during the charge/discharge process. Therefore, CU2-700 is suitable for making electrode materials to achieve a large charge storage capacity. At the same time, the results of EDS for CU2-700 (see Fig. 1d) indicate that N and O are successfully embedded into the carbon plates.

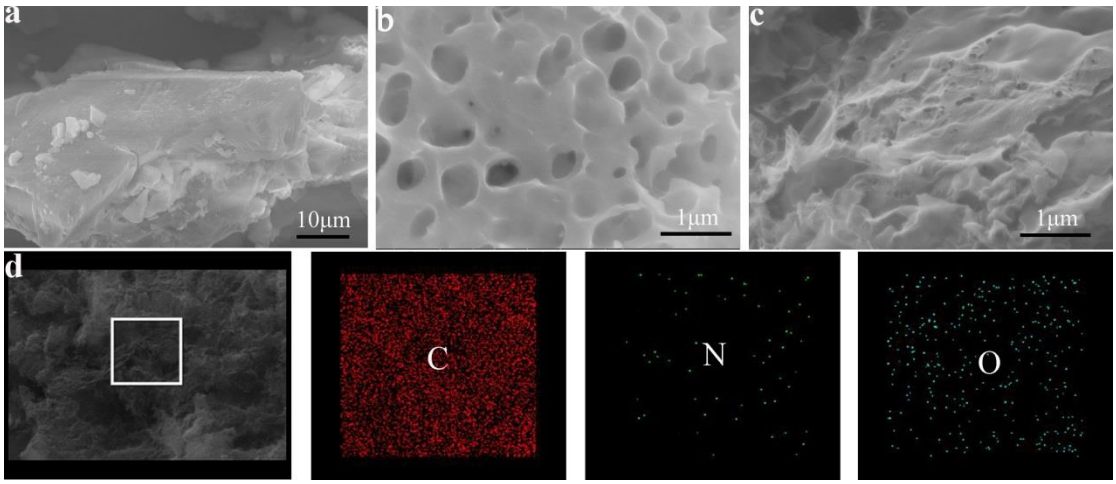

Figure 1. Typical SEM images of (a) precursor C; (b) C-700; (c) and CU2-700. (d) SEM-EDS of CU2-700.

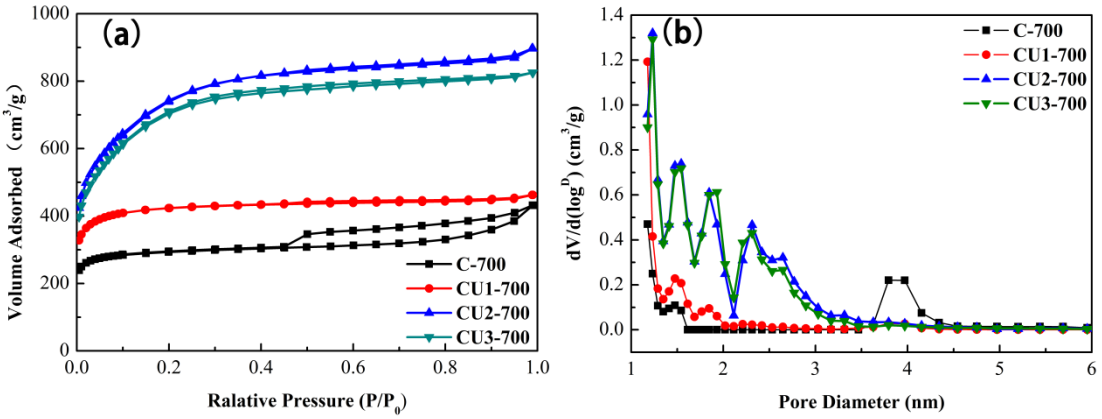

Figure 2. (a) Nitrogen sorption isotherms and (b) pore size distribution curves of C-700 and CUx-700.

The specific surface area and pore size distribution of materials are important factors in the field of carbon-based electrochemical capacitors. The performance of the N-PCs is further evaluated by nitrogen sorption isotherm measurements. The N_2 adsorption-desorption isotherms and the pore size distribution of the N-PCs are obtained by the quenched solid density functional theory (QSDFT) method (see Fig. 2). The isotherms of all the CUx-700 samples exhibit a typical type-I curve according to the IUPAC classification. This result indicates that all the CUx-700 (namely, CU1-700, CU2-700 and CU3-700) samples have characteristics of microporous materials. In addition, there are a certain number of

mesopores for CU2-700 and CU3-700 because their isotherms do not level off below the relative pressure of 0.2 [23,24]. However, the isotherm of C-700 reveals a typical type-IV curve with an apparent hysteresis loop at $p/p_o = 0.45$, implying that C-700 has only a mesoporous nature [23].The specific BET surface areas of C-700, CU1-700, CU2-700 and CU3-700 are 1136 $m^2\ g^{-1}$, 1643 $m^2\ g^{-1}$, 2628 $m^2\ g^{-1}$ and 2587 $m^2\ g^{-1}$ (according to Fig. 2a), respectively; while the pore volumes of these samples are obtained as 0.667, 0.717, 1.390 and 1.277 $cm^3\ g^{-1}$, respectively. These results demonstrate that doped N can increase the specific surface area of carbon materials. Fig. 2b shows the pore size distribution (PSD) of these samples. The pore distribution of C-700 is approximately 1.25 nm and 4 nm. The pore distribution of CU1-700 is from 1.2 to 2.0 nm. The CU2-700 and CU3-700 pores exhibit centralized pore distributions from 1.2 to 3.5 nm, and these pores include micropores (peaks at 1.25 nm and 1.5 nm) and small mesopores (peaks at 2.3 nm and 2.6 nm). These results indicate that the urea additive plays an important role in producing pores. A porous material with a high specific surface area is favourable for application as an active electrode material for energy storage due to quick mass charge transfer and ion diffusion. Consequently, CUx-700 is expected to produce a high specific capacitance.

The structures of the as-prepared samples were further studied by X-ray diffraction (XRD) and Raman spectroscopy. As shown in Fig. 3a, the XRD curves of all the samples reveal a broad peak at approximately 26° and a weak band at approximately 43°, attributed to the (002) and (100) planes, respectively. This result indicates that these samples have a typical amorphous graphitic structure [18]. Compared with C-700, the (100) peak intensity of CUx-700 is weaker, implying that its graphitization degree decreases. This phenomenon can also be seen from the SEM images (Fig. 1b and 1c). According to the Raman spectra (see Fig. 3b), there are two obvious peaks at approximately 1345 cm^{-1} (D band) and 1589 cm^{-1} (G band) for all the samples. The D band is related to the disordered and defective graphitic structure, while the G band is associated with the graphitic structure. Here, I_D and I_G represent the areas of the D and G peaks, respectively. The relative area ratio of I_D and I_G represents the graphitization degree of a carbon material [25]. The higher the I_D /I_G value is, the smaller the graphitization degree [26]. The obtained results show that the I_D/I_G values are 1.09, 1.18, 1.18, and 1.19 for C-700, CU1-700, CU2-700 and CU3-700, respectively. This result demonstrates that doped N increases the I_D/I_G value and reduces the graphitization degree, leading to disordered and defective carbon in the CUx-700 samples. Therefore, the above results also illustrate that CUx-700 is appropriate for electrode materials.

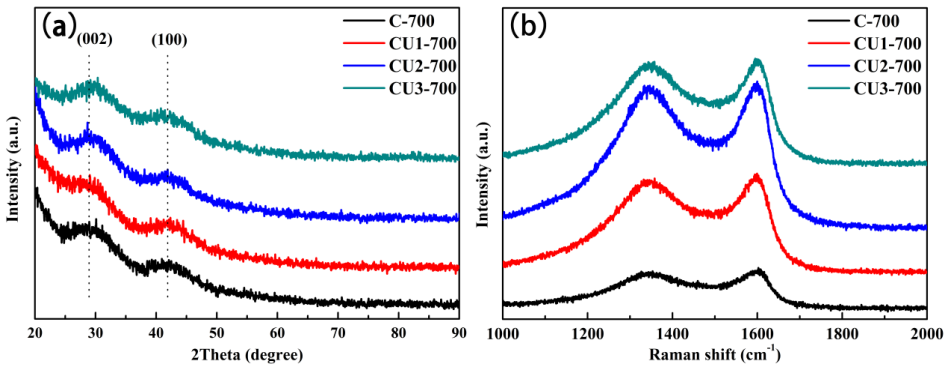

Figure 3. (a) XRD patterns and (b) Raman spectra of C-700 and CUx-700.

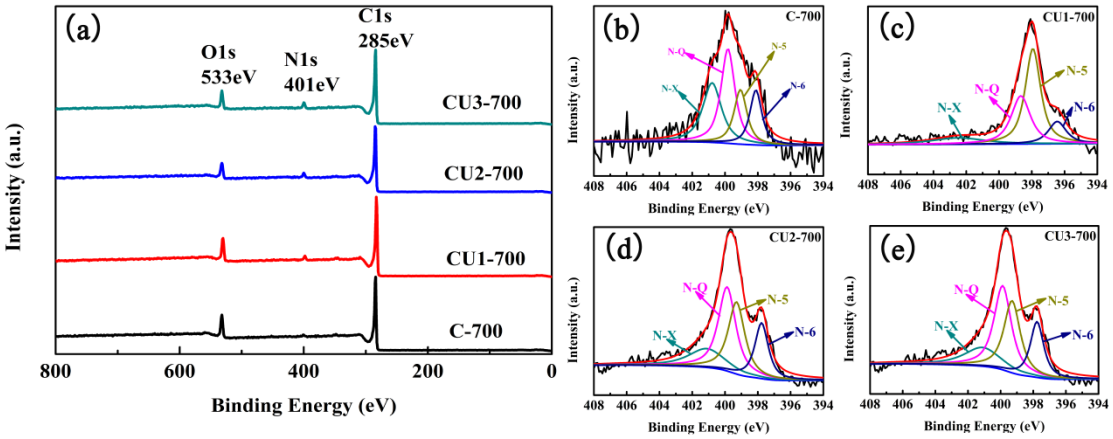

Figure 4. XPS spectra of as-prepared samples (a) and high-resolution XPS spectra of N 1s for (b) C-700; (c) CU1-700; (d) CU2-700; and (e) CU3-700.

To analyse the content and the types of nitrogen in the CUx-700 samples, X-ray photoelectron spectroscopy (XPS) measurements were carried out, and the results are presented in Fig. 4. As shown in Fig. 4a, all samples exhibit a predominant C 1s peak at 285 eV, a weak N 1s peak at 401 eV and an O 1s peak at 533 eV; no impurities are detected. According to Fig. 4b-4e and Table 1, the content of nitrogen in the samples increases with the content of doped urea. At the same time, the N 1s peak can be resolved into four individual peaks, attributed to pyridinic-N (N-6, ca. 398.5 eV), pyrrolic/pyridinic-N (N-5, ca. 399.7 eV), quaternary-N (N-Q, ca. 400.5 eV) and oxidized-N (N-X, ca. 402.6 eV), for all samples. This result indicates that nitrogen atoms are successfully incorporated into the carbon frameworks. According to previous studies [27,28], the electrochemical reaction takes place on charged N-5 and N-6 sites. Increasing the content of N-5 and N-6, therefore, can improve the electrochemical performance of supercapacitors. Meanwhile, N-Q and N-X can effectively enhance the conductivity of the porous carbon material and the cycling stability of supercapacitors. As shown in Table 1, compared with C-700, the contents of total N, N-5 and N-6 increased after doping with urea. Therefore, we infer that electrochemical performance will be improved for supercapacitors made by CUx-700 materials.

Table 1. Textural parameters of N for the samples.

Samples	Nitrogen content (wt.%)				
	Total	N-X	N-Q	N-5	N-6
		402.6 eV	401.5 eV	400.7 eV	398.7 eV
C-700	1.65	29.45	34.68	18.64	17.23
CU1-700	2.99	11.00	29.39	46.91	12.70
CU2-700	3.37	16.08	30.70	33.07	20.15
CU3-700	4.16	16.77	35.77	29.05	18.41

3.2. Electrochemical properties

In this section, we research the electrochemical properties of C-700 and CUx-700 in a three-electrode system in 6 M KOH aqueous electrolytes. Fig. 5a shows the CV curves of different carbon materials (C-700, CU1-700, CU2-700 and CU3-700) at a sweep rate of 50 mV/s in a potential range from -1 to 0 V (vs. Hg/HgO). The cyclic voltammetry (CV) curves of all the samples show a quasi-rectangular shape with broad and weak humps, which indicates the combination of electric double-layer capacitance (EDLC) and pseudo-capacitance related to the nitrogen-containing functional groups [29,30]. Clearly, the CU2-700 sample exhibits the largest area of the CV curve in the four samples. This result may be ascribed to the fact that CU2-700 has the largest specific surface area, the appropriate pore size and a certain degree of nitrogen content. Therefore, CU2-700 is the most promising material for supercapacitors among the four samples.

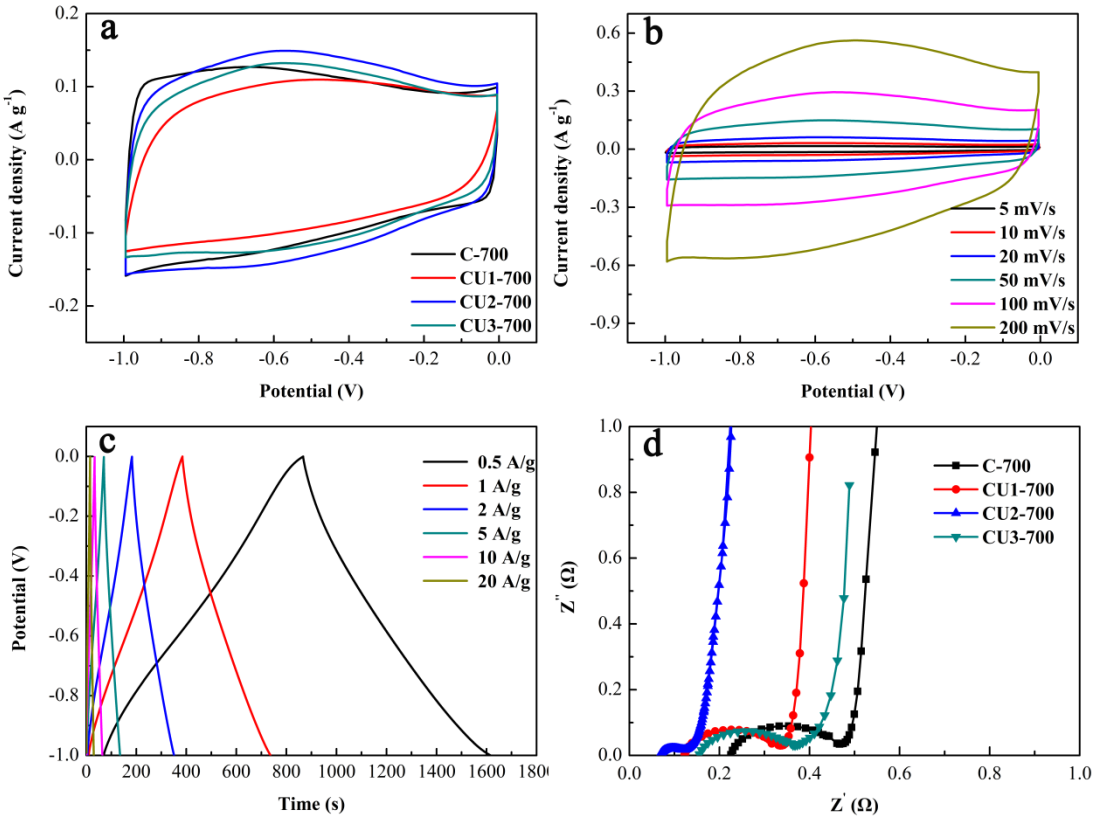

Figure 5. CV curves of as-prepared samples at a scan rate of 50 mV/s (a); CV curves of CU2-700 at different scan rates (b); GCD curves of CU2-700 at different current densities (c); and Nyquist plots of as-prepared samples (d).

To study the capacitive performance of CU2-700, its electrochemical properties were measured at different currents and different scan rates (see Fig. 5). The CV curves of CU2-700 maintain nearly symmetric and quasi-rectangular shapes when the potential scan rate increases from 5 to 200 mV s^{-1} (Fig. 5b). This result implies excellent ionic transfer and good double-layer capacitive performance [31]. The galvanostatic charge/discharge curves of CU2-700 at different current densities are presented in Fig.

5c. These curves display an almost isosceles triangular shape without an obvious IR drop at every current density, indicating ideal capacitive behaviour. The specific capacitances are calculated as 373, 351, 336, 321, 306 and 288 F/g, respectively, corresponding to current densities of 0.5, 1, 2, 5, 10 and 20 A/g (approximately 77% capacitance retention) from the discharge curves. Compared to the literature (see Table 2), this proposed supercapacitor has a higher specific capacitance value. For example, the specific capacitance of a supercapacitor made by Pueraria as a C source [33] showed 250 F g^{-1} and that by bagasse [38] was only 320 F/g at 0.5 A/g current density in 6 M KOH. This result demonstrates that cycas leaves can be used as a good biomass C source for supercapacitors.

Table 2. Comparison of the specific capacitance of CU2-700 with that of other reported biomass C sources.

Biomass carbons	Specific capacitances (F/g)	Current densities (A/g)	Electrolyte	Ref.
Cycas leaves	373	0.5	6 M KOH	This work
Cycas leaves	351	1	6 M KOH	This work
Nature casings	307.5	0.5	6 M KOH	32
Pueraria	250	0.5	6 M KOH	33
Ant powder	576	1	6 M KOH	34
Water chestnut	346	0.5	6 M KOH	35
Willow catkin	292	1	6 M KOH	36
Poplar catkin	314.6	0.5	6 M KOH	37
Bagasse	320	0.5	6 M KOH	38

Electrochemical impedance spectroscopy (EIS) was employed to further investigate the ion diffusion and transport kinetics. Fig. 5d displays the Nyquist plots of all carbon specimens. According to Fig. 5d, all the samples show steep linear curves in the low-frequency region, meaning an ideal capacitive performance [39,40]. The radius of the semicircle in the high-frequency region represents charge transfer resistance (R_{ct}) in electrochemistry. Fig. 5d shows that doped N can reduce R_{ct} for all the samples, and the R_{ct} value of CU2-700 is the smallest. This result indicates that ion transport is the easiest and fastest in CU2-700. From Fig. 5d, it can also be found that the internal resistance (R_S) is 0.22 Ω, 0.12 Ω, 0.068 Ω and 0.15 Ω, respectively, corresponding to C-700, CU1-700, CU2-700 and CU3-700. It is thus clear that doped N can reduce the R_S value of carbon materials, and R_S of CU2-700 is minimal. Decreasing R_S enhances the electrode conductivity [41]. The above results indicate that CU2-700 has lower R_{ct} and R_S, further demonstrating that CU2-700 has good electrochemical performance.

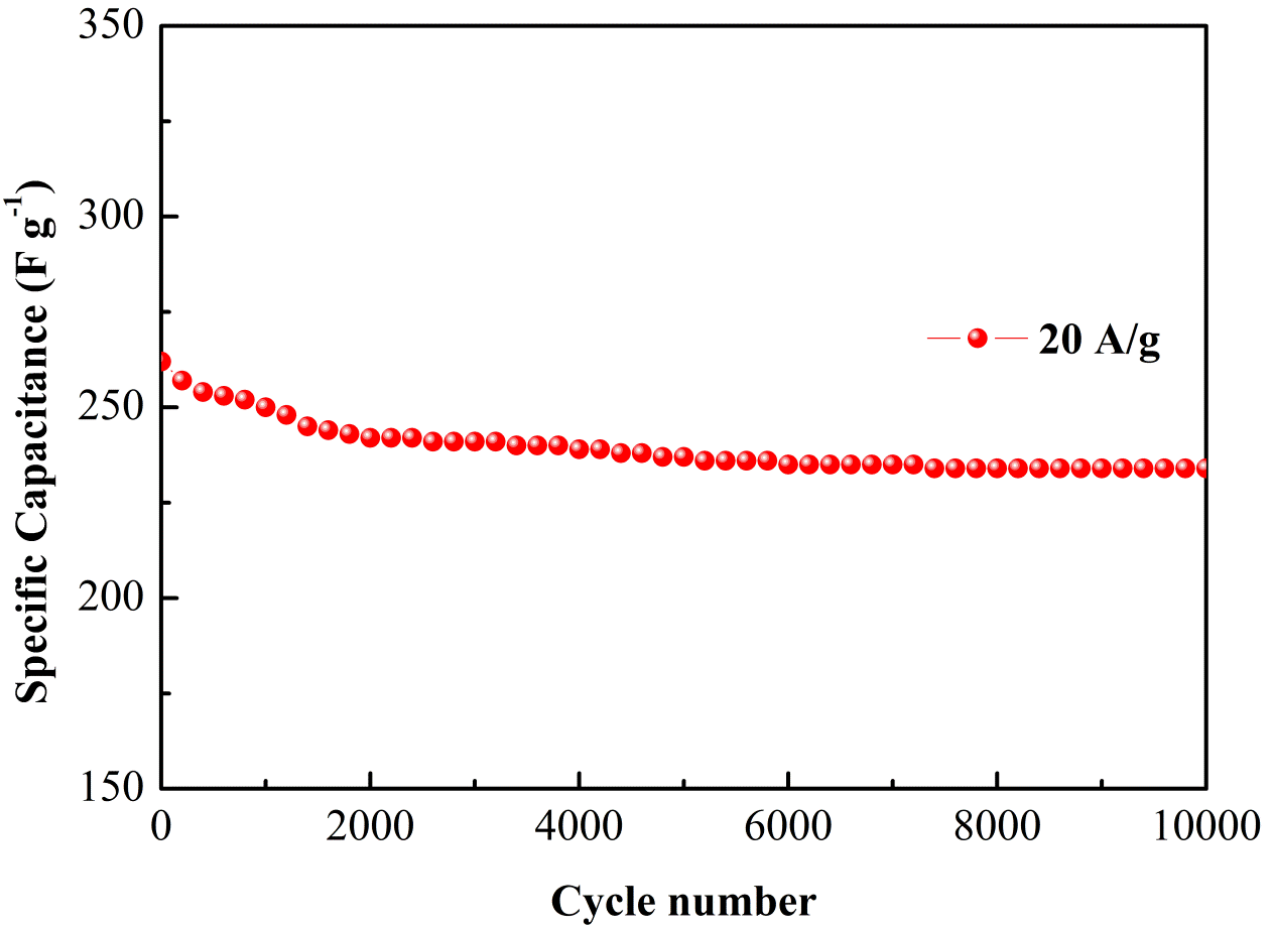

Figure 6. Cycling performance of CU2-700.

The cycle life is one of the most important features of supercapacitors. The long-term cycling stability of CU2-700 was tested using galvanostatic charge/discharge at 20 A g^{-1} (see Fig. 6). As shown in Fig. 6, the initial capacitance of CU2-700 is approximately 262 F/g, and the capacitance is still 234 F/g (exceeding 89% of the initial capacitance) after the 10000th cycle. This result indicates that CU2-700 has excellent stability and high capacitance retention.

In addition, a two-electrode symmetric supercapacitor was assembled in a 6 M KOH aqueous electrolyte. Fig. 7a shows its CV curves at different scan rates. The CV curves indicate a double-layer capacitive performance, even when the scan rate increases to 200 mV/s. Fig. 7b shows the GCD curves of the symmetric cell with the CU2-700 electrodes at a current density ranging from 0.5 to 10 A/g. All the curves show a regular symmetric triangular shape, implying good electrochemical charge and discharge reversibility. The specific capacitances of CU2-700 at different current densities are shown in Fig. 7c. The specific capacitances are 260 F/g at 0.5 A/g and 203 F/g at 10 A/g (78% of the capacitance retention).

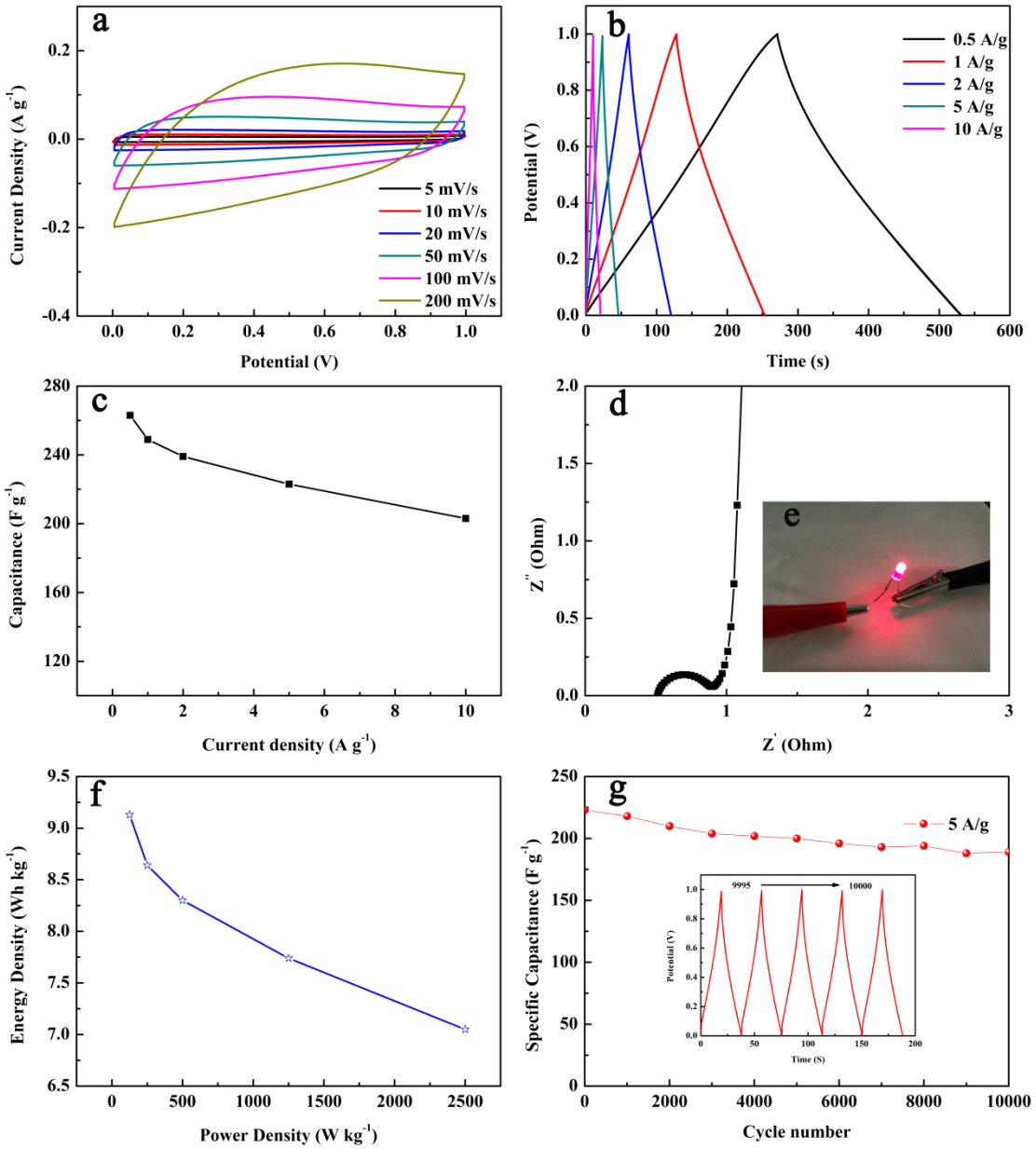

Figure 7. Electrochemical performance of CU2-700 in a two-electrode system. a: CV curves at various scan rates of 5–200 mV/s; b: GCD curves tested at 0.5 – 10 A/g; c: specific capacitance at different current densities; d: Nyquist plots; e: LED lit up by a device of two supercapacitors connected in series; f: a curve of energy density vs. power density; g: capacitance retention over 10000 cycles.

Fig. 7d shows a Nyquist plot of the symmetric cell of CU2-700. The Nyquist plot shows a small semicircle in the high-frequency region and the vertical part of the curve in the low-frequency region, which suggests that it has good capacitive behaviour. An energy storage device with two supercapacitors connected in series was fabricated. Such a simple energy storage device could power a commercial red light-emitting diode (LED), as shown in Fig. 7e. The energy density of the CU2-700 capacitor is approximately 9.13 W h/kg at a power density of 125 W/kg (see Fig. 7f). Cycling stability is a critical parameter for supercapacitors in practical applications. As shown in Fig. 7g, CU2-700 shows an

excellent cycle life; its specific capacitance is 189 F/g after 10000 charge/discharge cycles at a current density of 5.0 A/g, which is approximately 85% of the initial specific capacitance.

4. CONCLUSIONS

Considering the worldwide abundance and recyclability of cycas, its leaves can be widely used as a novel biomass source for producing porous carbons. Therefore, we propose a simple route to fabricate N-doped porous carbon by using cycas leaves as a carbon source and urea as a nitrogen source. The experimental results show that cycas leaves are a good kind of biomass carbon, and doped N helps to reduce R_{ct} and R_S and increase the electrochemical reaction sites of the porous carbons. Among three prepared kinds of CUx-700, CU2-700 exhibits the best electrochemistry performance, owing to its hierarchical porous structure with a very high specific surface area of 2628 m^2 g^{-1} and a large pore volume of 1.39 cm^3 g^{-1}. A supercapacitor made by CU2-700 displays a high specific capacitance of 373 F g^{-1} at 0.5 A g^{-1} and excellent cycling stability (approximately 89% of the initial capacitance retention after 10000 cycles at 20 A g^{-1}). Furthermore, the as-assembled CU2-700 supercapacitor with a 6 M KOH electrolyte in a two-electrode system exhibits an excellent specific capacitance of 260 F/g at 0.5 A/g and perfect long-term cycling stability. Its capacitance retention is approximately 85% of the initial capacitance, even after 10000 charge-discharge cycles at 5 A/g. It also achieved a high energy density of approximately 9.13 W h/kg at a power density of 125 W/kg. This facile biomass-based approach provides an alternative route for preparing N-doped porous carbon that can be a promising candidate for supercapacitor applications in the future.

ACKNOWLEDGEMENTS
This work was supported by the National Natural Science Foundation of China (U1501242 and 51671062), the Guangxi Collaborative Innovation Centre of Structure and Property for New Energy and Materials (2012GXNSFGA06002), the Guangxi Science and Technology Project (AD17195073), the Guangxi Major Science and Technology Special Project (AA17202030-1) and the Guangxi Key Laboratory of Information Laboratory Foundation (161002-Z, 161002-K and 161003-K).

References

1 F. X. Ma, L. Yu, C. Y. Xu, X. W. Lou, *Energy Environ. Sci.,* 9 (2016) 862-866.
2 X. Zhou, L. Yu, X. W. Lou, *Adv. Energy Mater.,* 6 (2016) 1600451.
3 Q. Wang, J. Yan, Z. Fan, *Energy Environ. Sci.,* 9 (2016) 729-762.
4 Y. Zeng, Y. Han, Y Zhao, *Adv. Energy Mater.,* 5 (2015) 1402176.
5 D. S. Yu, K. L. Goh, H. Wang, *Nat. Nanotechnol.,* 9 (2014) 555-562.
6 J. Yan, Q. Wang, T. Wei, Z. J. Fan, *Adv. Energy Mater.,* 4 (2014) 1300816.
7 E. Frackowiak, F. Béguin, *Carbon,* 39 (2001) 937-950.
8 B. Li, F. Dai, Q. F. Xiao, L. Yang, C. M. Zhang, M. Cai, *Energy Environ. Sci.,* 9 (2016) 102-106.
9 M. Cakici, R. Kakarla, F. Alonso-Marroquin, *Chem. Eng. J.,* 309 (2017) 151-158.
10 X. J. Wei, S. G. Wan, S. Y. Gao, *Nano Energy,* 28 (2016) 206-215.
11 C. Y. Xiong, T. H. Li, A. L. Dang, T. K. Zhao, H. Li, H. Q. Li, *J. Power Sources,* 306 (2016) 602-

610.
12 A. Ramadoss, K. Y. Yoon, M. J. Kwak, S. I. Kim, S. T. Ryu, J. H. Jang, *J. Power Sources,* 337 (2017) 159-165.
13 B. Cardoso, A. S. Mestre, A. P. Carvalho, Pires J, *Ind. Eng. Chem. Res.*, 47 (2008) 5841-5846.
14 M. A. Lillo-Ródenas, D. Lozano-Castelló, D. Cazorla-Amorós, A. Linares-Solano, *Carbon,* 39 (2001) 751-759.
15 J. Paraknowitsch, A. Thomas, *Energy Environ. Sci.,* 6 (2013） 2839-2855.
16 K. N. Wood, R. O'Hayre, S. Pylypenko, *Energy Environ. Sci.,* 7 (2014) 1212-1249.
17 K. Mamtani, U. S. Ozkan, *Catal. Lett.*, 145 (2015) 436-450.
18 K. Xiao, L. X. Ding, H. B. Chen, S. Q. Wang, X. H. Lu, H. H. Wang, *J. Mater. Chem. A,* 4 (2015) 372–378.
19 Y. Q. Zhang, X. Liu, S. Wang, S. L. Dou, L. Li, *J. Mater. Chem. A,* 4 (2016) 10869-10877.
20 L. Zhang, L. Xu, Y. G. Zhang, X. Zhou, L. T. Zhang, A. Yasin, L. L. Wang, K. K. Zhi, *RSC Adv*., 8 (2018) 3869-3877.
21 S. Yan, J. J. Lin, P. Liu, Z. C. Zhao, J. Lian, W. Chang, L. Yao, Y. R. Liu, H. L. Lin, S. Han, *RSC Adv.,* 8 (2018) 6806-6813.
22 S. S. Qu, J. F. Wan, C. C. Dai, T. Y. Jin, F. W. Ma, *J. Alloys Compd.,* 751 (2018) 107-116.
23 K. Sing, *Pure Appl. Chem.,* 57 (1985) 603-619.
24 F. Rodriguezreinoso, J. Martinmartinez, C. Pradoburguete, *J. Chem. Phys.,* 91 (1987) 1293-1311.
25 H. L. Wang, Z. W. Xu, A. Kohandehghan, Z. Li, *ACS Nano,* 7 (2013) 5131-5141.
26 A Ferrari, J. Robertson, *Phys. Rev. B,* 61 (2000) 14095-14107.
27 F. Kapteijn, J. A. Moulijn, S. Matzner, H. P. Boehm, *Carbon,* 37 (1999) 1143-1150.
28 L. J. Zhang, Z. X. Su, F. L. Jiang, L. L. Yang, J. J. Qian, Y. F. Zhou, W. M. Li, M. C. Hong, *Nanoscale,* 6 (2014) 6590-6602.
29 Q. Wang, J. Yan, Y. B. Wang, T. Wei, M. L. Zhang, X. Y. Jing, Z. J. Fan, *Carbon,* 67 (2014) 119-127.
30 R. B. Rakhi, W. Chen, D. Cha, H. N. Alshareef, *Adv. Energy Mater.,* 2 (2012) 381-389.
31 C. C. Ma, X. H. Shao, D. P. Cao, *J. Mater. Chem. A,* 22 (2012) 8911-8915.
32 Z. Y. Xu, Y. Li, D. D. Li, D. W. Wang, J. Zhao, Z. F. Wang, H. H. Zhang, *Appl. Surf. Sci.*, 444 (2018) 661-671.
33 X. L. Han, H. X. Jiang, Y. Zhou, W. F. Hong, Y. F. Zhou, P. Gao, R. Ding, E. H. Liu, *J. Alloys Compd.*, 744 (2018) 544-551.
34 G. Y. Zhao, C. Chen, D. F. Yu, L. Sun, C. H. Yang, H. Zhang, Y. Sun, M. Yu, *Nano Energy,* 47 (2018) 547-555.
35 H. M. Wei, J. Chen, N. Fu, H. J. Chen, H. L. Lin, S Han, *Electrochim. Acta,* 266 (2018) 161-169.
36 Y. J. Li, G. L. Wang, T. Wei, Z. J. Fan, P. Yan, *Nano Energy,* 19 (2016) 165-175.
37 X. L. Su, M. Y. Cheng, L. Fu, J. H. Yang, X. C. Zheng, X. X. Guan, *J. Power Sources,* 362 (2017) 27-38.
38 H. B. Feng, H. Hu, H. W. Dong, Y. Xiao, Y. J. Cai, B. F. Lei, Y. L. Liu, M. T. Zheng, *J. Power Sources,* 302 (2016) 164-173.
39 D. C. Guo, J. Mi, G. P. Hao, W. Dong, G. Xiong, W. C. Li, A. H. Lu, *Energy Environ. Sci.,* 6 (2013) 652-659.
40 M. Biswal, A. Banerjee, M. Deo, S. Ogale. *Energy Environ. Sci.,* 6 (2013) 1249-1259.
41 G. X. Zhang, Y. M. Chen, Y. G. Chen, H. B. Guo, *Mater. Res. Bull.*, 102 (2018) 391–398.